Unified Network Model for Adsorption–Desorption in Systems with Hysteresis

Pavol Rajniak and Miroslav Soós
Dept. of Chemical and Biochemical Engineering, Slovak Technical University, 812 37 Bratislava, Slovakia

Ralph T. Yang
Dept. of Chemical Engineering, University of Michigan, Ann Arbor, MI 48109

The problem of equilibrium and kinetics for adsorption–desorption of condensable vapors in porous media is studied experimentally and theoretically. For adsorption, the network model for diffusion based on pore blocking theory with percolation (in the network) added by effective medium approximation is further improved. A new predictive model based on properties of the Bethe lattices is proposed to account for the existence of liquid-filled ''blind'' pores that result in a decrease in the total diffusion rate. For desorption, a new ''shell and core'' (or shrinking core) representation of the network model is proposed. Information from adsorption–desorption equilibria is needed to compute the thickness of the shell in which desorption/evaporation occurs for concentrations higher than the percolation threshold. These models form a unified equilibrium-kinetics theory for gas-porous solid systems that exhibit hysteresis. The models are applied to the systems silica gel-water vapor and Vycor glass-nitrogen. Concentration-dependent Fickian diffusivities for these systems have been measured for both adsorption and desorption branches. The adsorption model successfully predicts the experimental data with a maximum in diffusivity. The desorption model correctly predicts the concentration dependence of diffusivity with a steep minimum at the percolation threshold.

Introduction

The problem of predicting diffusion rates of adsorbable vapors in porous media in the range of pressure where capillary condensation occurs is a significant one for the design and operation of adsorbers, dryers, catalytic reactors, membrane separators, and so on. Although many aspects of the diffusion/transport process are understood in principle (Sahimi, 1995), the important role of capillary condensation and evaporation has been largely neglected due to difficulties in separating the contributions from different transport mechanisms.

For adsorption and desorption of condensable vapors, the vapor in the adsorbent exists as adsorbed molecules on the solid surface, condensate in fine pores and as vapor in the voids. During adsorption at low partial pressures, monolayer adsorption plays the major role. At higher partial pressures, the role of multilayer adsorption becomes important and simultaneously capillary condensation in the finer pores begins. Capillary condensation increases with increasing relative pressure, and eventually the entire pore volume becomes filled by capillary condensate. During desorption, as the relative pressure is reduced, systems in which capillary condensation occurs generally show hysteresis, that is, in a particular pressure range more vapor remains adsorbed during desorption than was adsorbed during the initial adsorption process. Classical explanations of hysteresis based on single pores (such as Everett, 1967; Gregg and Sing, 1982) cannot satisfactorily explain some important experimental observations, such as the higher-order adsorption–desorption scanning curves. Models that treat the pore system as an interconnected network have been developed more recently. These models attribute hysteresis to pore blocking where the emptying of a

Correspondence concerning this article should be addressed to R. T. Yang.

large pore filled with capillary liquid has to be preceded by the emptying of its smaller neighbors (Mason, 1988; Parlar and Yortsos, 1988; Seaton, 1991; Li et al., 1991; Lilly et al., 1993; Rajniak and Yang, 1993, 1994). Hence, the primary desorption is a connectivity-related phenomenon. Such phenomena can be described best by percolation theory (Broadbent and Hammersley, 1957).

The percolation model for primary desorption is not in complete agreement with the experimental data shown in Figure 1a, because the initial part of the real desorption isotherm is not horizontal as described by the theory and shown in Figure 3a. There are various explanations for this fact: decompression of the liquid phase (Mason, 1988) and nucleation effects (Parlar and Yortsos, 1989). Liu et al. (1993) carried out extensive Monte Carlo simulations of the primary desorption and have shown that the finite size of the microparticles is important and the surface clusters must be taken into account. The desorption process is then related to invasion percolation (Wilkinson and Willemsen, 1983), the main difference being that here the invading phase (vapor in this case) enters from the whole surface of the system, rather than from just one face (Guyer and McCall, 1996; Page et al., 1993).

The equilibrium behavior of capillary condensate is relatively well understood, but its dynamic behavior has not been studied in the works cited above. Various experimental methods used to determine the mass transport rates in the capillary condensation regime (Rhim and Hwang, 1975; Tamon et al., 1981; Toei et al., 1983; Eberly and Vosberg, 1965) and theoretical approaches explaining the experimental results (Carman, 1952; Flood et al., 1952; Gilliand et al., 1958; Kapoor et al., 1989) have appeared in the literature. Most of them are discussed in our previous work (Rajniak and Yang, 1996).

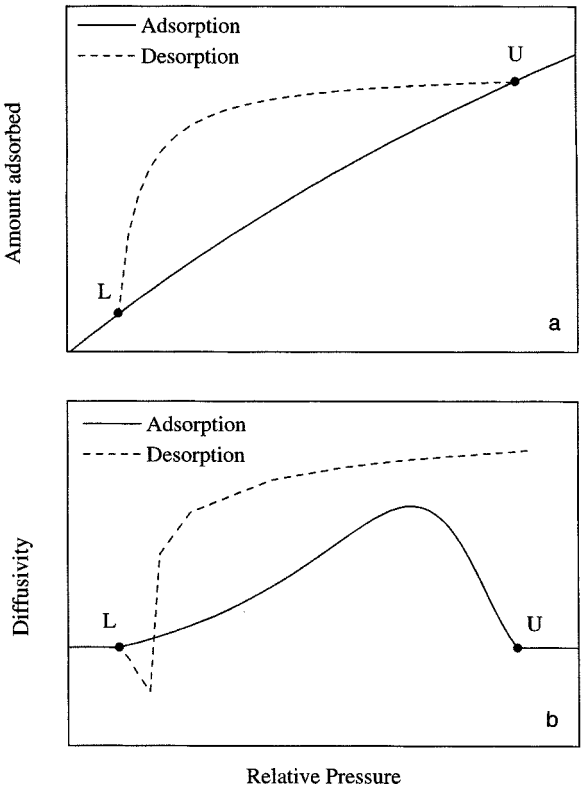

Figure 1. Experimental hysteresis dependent adsorption-desorption equilibria and kinetics.

(a) Equilibria; L = lower limiting point, U = upper limiting point of the hysteresis loop; (b) kinetics.

Like in adsorption-desorption equilibria, hysteresis has also been reported for the diffusion rates or kinetics in the capillary condensation region. Hysteresis in both equilibria and kinetics are illustrated, respectively, in Figures 1a and 1b. The concentration dependence of diffusivity exhibits a maximum during adsorption and a minimum during desorption. Interestingly, the maximum is located near the upper closure point (U) of the hysteresis loop (Chen and Yang, 1993), while the minimum appears near the lower closure point (L). The adsorption and desorption branches coincide only in the region of surface diffusion, that is, at low partial pressures. Such concentration dependence is typically seen in gravimetric measurements for rates of adsorption and desorption when the results are fitted by the transient diffusion equation (Fick's second law) with a constant diffusivity (Kärger and Ruthven, 1992; Rajniak and Yang, 1996). Mass transport in the porous material is a complex combination of gaseous diffusion, surface diffusion, capillary condensation/evaporation, and flow of liquid condensate. Evaluation of such a complicated process using diffusion equation with a constant diffusivity is only a mathematical simplification for the purpose of comparing rates at various concentrations during adsorption and desorption. Literature reports on hysteresis in the kinetics in adsorption-desorption include the study of capillary condensation flow of toluene in Vycor glass (Abeles et al., 1991), gravimetric measurements of the kinetics of isothermal adsorption and desorption of isopropanol in Vycor glass (Haynes and Miller, 1982), multilayer diffusion and capillary condensation of propylene in supported alumina films (Uhlhorn et al., 1992), permeabilities in Vycor glass (Lee and Hwang, 1986), and isothermal transport of liquids in partially saturated packed beds of glass spheres (Büssing et al., 1996).

Literature reports that are of particular interest to this work are the theory on preparation of supported catalysts (Neimark et al., 1981), moisture transport in microporous substances (Radjy, 1974), study of drying by NMR imaging (Maneval et al., 1991), and determination of moisture diffusivity in porous media using concentration profiles (Pel et al., 1996). The models used in these studies represent the classic continuum approach (Sahimi et al., 1990). Most of these works are restricted to the idealized case of a single pore size. The complexities caused by the pore-size distribution and by the network effects were not considered. In the continuum models, the porous medium is treated as a continuum within which the properties of the fluid and solid phases are defined as smooth functions of time and positions. Continuum models are often not adequate for systems consisting of phases that differ appreciably from one another in their effective properties (Sahimi et al., 1990).

There have been only a few studies on kinetics using network models where phase changes are included (Daian, 1992; Yortsos et al., 1993; Prat, 1993, 1995; Laurindo and Prat, 1996; Li and Yortsos, 1995; Rajniak and Yang, 1996). Daian (1992) examined various methods for computing moisture diffusion rates. The interactions between vapor diffusion and liquid

transport are discussed based on the network theory. Some experimental results seem to indicate that the actual role of vapor diffusion is strongly influenced by its interaction with the liquid phase through condensation and evaporation. Prat and coworkers studied evaporation in porous media (Prat, 1993, 1995; Laurindo and Prat, 1996). They conclude that evaporation belongs to the invasion percolation type. The main difference between evaporation and standard invasion percolation lies in the erosion of the disconnected liquid clusters that form as a result of the growth of the invading vapor phase. As phase change takes place at the boundary of these disconnected clusters, they can be invaded in evaporation while they are generally considered as trapped in standard invasion percolation. Experimental and simulated phase distributions (Laurindo and Prat, 1996) for the case with stabilizing gravity forces show a sharp boundary between the liquid and vapor phases.

In our recent work (Rajniak and Yang, 1996), a network model was formulated for predicting effective Fickian diffusivities of condensable vapors in porous media where capillary condensation and adsorption-desorption hysteresis occur. The model unifies the equilibrium theory based on the pore-blocking interpretation of hysteresis in the interconnected network of pores and the percolation model of mass transport in the network with randomly interspersed regions for capillary condensation and surface flow. In the present work, we briefly summarize the main concepts of the equilibrium theory for adsorption-desorption systems with hysteresis (Mason, 1988; Rajniak and Yang, 1993, 1994) based on the pore-blocking theory and percolation theory in the Bethe tree network. Next, the network model for both adsorption and desorption kinetics is developed for the idealized case of the infinite media. Modifications of the theory necessary for real systems with finite dimensions of the network are then proposed. For adsorption, a modification is proposed for the computation of ''blind'' liquid-filled pores. The derivation is based again on the Bethe tree approximation of the pore network structure. The only parameter in the proposed model is connectivity, which can be obtained independently. The improved model predicts the concentration dependence of the effective diffusivity for systems with a maximum diffusivity. For desorption kinetics, a model is proposed for computing the descending branch of the concentration dependence of effective diffusivity for relative pressures higher than that corresponding to the percolation threshold. The proposed model is based on the ''shrinking core'' (Sahimi et al., 1990; Lee and Aris, 1985; Brunovská et al., 1985; Markos et al., 1987). In order to compare the predictions of the proposed models with experimental data, a complete set of concentration-dependent equilibrium-diffusion data is obtained for the system Vycor glass-nitrogen.

Theoretical Considerations

We consider the adsorption-desorption process of a condensable vapor in a porous adsorbent. In Figure 1a the adsorption-desorption equilibria for the process are shown. At relative pressures below point L, the lower closure point of the hysteresis loop, only surface adsorption occurs. The position of point L is characteristic of each sorbate-sorbent pair (such as, Naono and Hakuman, 1993; Burgess et al., 1989). Mass transport rates in this region are contributed by gaseous diffusion and surface diffusion. Mass transport rates in this region are the same for both adsorption and desorption, and the study of the kinetics in this region is out of scope of this work (Kärger and Ruthven, 1992; Yang, 1987).

Above point U, the upper closure point of the hysteresis loop, all pores become filled with capillary condensate. The position of point U depends on the pore-size distribution of the adsorbent. If point U lies below the saturation pressure of the adsorptive, then it is presumed that the solid has no pores of radii greater than that corresponding to the closure point. Adsorption beyond this pressure is related to the change of curvature of menisci freely accessible to the vapor and the compression of liquid condensate in the pores (Liu et al., 1993). On the other hand, when decreasing the pressure in the region above point U, a negative pressure is produced and this decompression reduces the density of liquid condensate (Mason, 1988). Transport of liquid condensate in the region above point U can then occur only by hydraulic pressure, and, under usual conditions of adsorption experiments, this flow is much smaller than the capillary condensate flow. During adsorption at point L, the condensation pressure is reached in the finest pores and the pores are filled with a liquidlike phase. The extent of capillary condensation increases with increasing pressure, and, at point U, the entire pore volume is filled by capillary condensate.

In this study we are interested in the mass transport rate in the region of capillary condensation, that is, in the region between the limiting points of the main hysteresis loop L and U.

Adsorption-desorption equilibria for infinite systems

The pore blocking theory (Mason, 1988; Rajniak and Yang, 1993, 1994) was developed directly for the capillary condensation domain, and it describes the adsorption-desorption equilibria for relative pressures $x^L < x < x^U$. Following the pore blocking theory, a porous material consists of a number of pores connected together in a network in which we distinguish sites (pore bodies) from bonds (pore throats). The individual sites are connected via bonds. The average number of bonds to each site is defined as connectivity C. The characteristic dimension of the site or of the bond r can be related to the macroscopic Kelvin equation for capillary condensation. Thus, at any value of relative pressure x, the process may be uniquely parametrized by the characteristic dimension r. Another important function is q, the probability that the site is filled by capillary condensate at relative pressure x. Similarly p is the probability that the bond is filled at the relative pressure x. Under the assumptions that the capillary condensation phenomenon controls the equilibrium of the sorption process between points L and U, and that the volume of capillary condensed liquid is primarily associated with the cavities, the adsorption process is represented by an increase of $q = 0$ at $x = x^L$ to $q = 1$ at $x = x^U$. On the other hand, the desorption process is represented by a decrease of $p = 1$ at $x = x^U$ to $p = 0$ at $x = x^L$.

The probabilities p and q are related through connectivity C by (Mason, 1988; Rajniak and Yang, 1993)

$$q = p^C \tag{1}$$

To relate q and p to a, the amount adsorbed on the sorption isotherms, the variable S must be introduced. S, the fraction of pores filled, is related to the adsorbed amount by the expression

$$S = \frac{a - a^L}{a^U - a^L} \tag{2}$$

The amount adsorbed a during adsorption or desorption is a function of the relative pressure x via the adsorption or desorption isotherm, that is,

$$a_A = f(x) \tag{3a}$$

$$a_D = f(x) \tag{3b}$$

For the primary adsorption process (the subscript A is for primary adsorption and the subscript D for primary desorption), the fraction of pores filled by capillary condensation is

$$S_A = q \tag{4}$$

It is worth noting that S_A is not dependent on connectivity C. Pore blocking does not play any role in adsorption equilibria. When a porous material is filled by adsorption, all of the pores are equally accessible. Even if the pore becomes isolated from the bulk vapor, it can still fill by condensing vapor from adjacent pores that can then refill from the bulk vapor.

For primary desorption, the hysteresis of capillary condensed vapor can be explained by pore-blocking effects, where a pore cannot empty until at least one of its neighbors has emptied. This effect depends in principle on the interconnections and the interconnectedness of the pore network. The model frequently used for the interconnectedness is the Bethe tree shown in Figure 2. The advantage of using the Bethe tree is that the description of its behavior can be carried out analytically. Bethe trees can give simplified expressions for several properties of the porous medium, while retaining most features of percolation theory (Sahimi, 1993; Kainourgiakis et al., 1998).

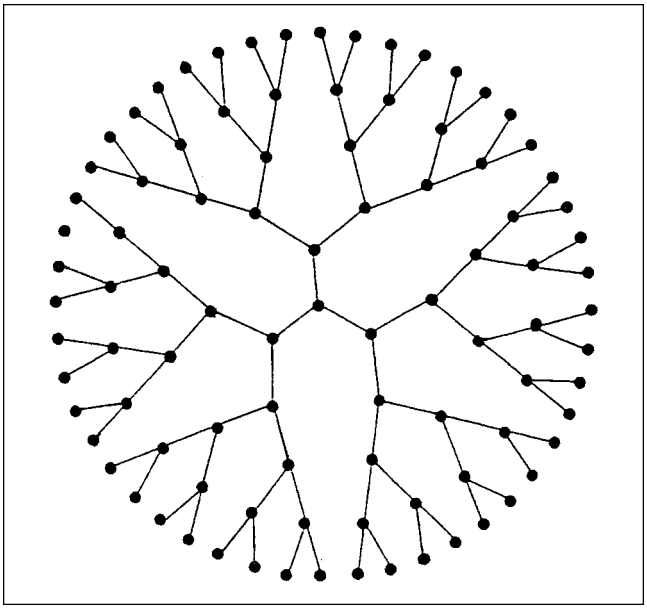

Figure 2. Bethe lattice with connectivity $C = 3$.

The analysis given here uses percolation theory (Stauffer and Aharony, 1992; Sahimi, 1994, 1995) with the restriction to a Bethe tree network. During the primary desorption process, whether a site remains full or empty depends on whether one of its bonds is connected to the vapor and at the same time can also be emptied. At some stage during primary desorption, at some value of p, the probability that a bond into a site is connected to the vapor is v. The fraction of the pores filled during primary desorption S_D at probabilities p and v can be computed via Eqs. 5 and 6 derived by Mason (1988)

$$S_D = (vp + 1 - v)^C \tag{5}$$

where

$$(vp + 1 - v)^{(C-1)} = 1 - v \tag{6}$$

Combining Eqs. 1–6 and knowing connectivity C, we can compute for any relative pressure x the amount adsorbed during desorption a_A, or during desorption a_D, and the corresponding fractions of pores filled S_A or S_D, and the probabilities q and p.

Figure 3a shows the theoretical primary desorption isotherm computed from Eqs. 1–6 assuming $C = 3$. The ini-

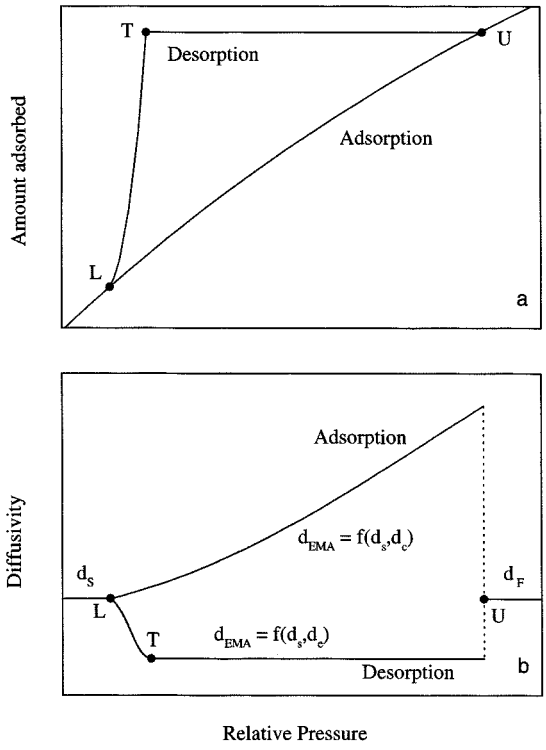

Figure 3. Theoretical hysteresis-dependent adsorption-desorption equilibria and kinetics.

(a) Equilibria, T = percolation threshold; (b) kinetics.

tial part of the theoretical desorption isotherm (between points U and T) is a horizontal line. In fact, the theoretical relations 5 and 6 give values $S_D = 1$ for all values of p greater than p^T, where

$$p^T = \frac{(C-2)}{(C-1)} \tag{7}$$

is the value of probability p at the percolation threshold T of the desorption process.

Along this desorption branch, there is theoretically no desorption. Desorption should begin only at point T, the percolation threshold for primary desorption, when there is a sufficient number of bonds in which the adsorbate is below its condensation pressure (and thus is present as either metastable liquid or vapor) and, consequently, a sufficient number of vapor connections in the porous network and desorption from the bulk of the adsorbent can start.

The primary adsorption process in the capillary condensation region can be treated as a classic site percolation problem. Pores with different dimensions are randomly distributed in the pore space. In this case pore sites of the network are filled by capillary condensate with probability q and partially filled by surface adsorption with probability $1-q$. However, percolation characteristics of the primary adsorption are not important for description of the equilibrium behavior of the process, because whether a particular site is filled by capillary condensation depends only on its characteristic dimension. The percolation properties of the primary adsorption are of particular interest for the kinetic behavior of the process.

The primary desorption equilibrium problem belongs to the group of bond percolation problems, because the emptying of the pore sites is determined by the bonds connections. Connectivity of the network plays a dominant role in the description of the process. The theoretical model using Bethe tree is developed for the infinite system and the clusters at the surface of the system cannot be taken into account. Between points T and U starting with a filled system, p is progressively reduced until at the critical value p^T, the system starts to empty. This occurs at the critical percolation probability p^T. For an infinite system, there is no desorption until the percolation threshold is reached and the desorption isotherm has a discontinuity in slope at the threshold.

Adsorption-desorption kinetics for infinite systems

Mass transport in the capillary condensation region is a complex phenomenon. The conditions under which capillary condensation occurs are also those under which significant surface diffusion is expected. Study of this phenomenon is therefore complicated by the difficulty of separating the contributions from the various transport mechanisms. Fortunately, vapor-flow contribution is found to be negligible under these conditions. Vapor-phase transport is in this case usually orders of magnitude smaller than the surface flow because of the relatively small amount of molecules in the vapor phase compared to that in the adsorbed phase (Haynes and Miller, 1982; Abeles et al., 1991). As soon as a pore is filled with condensate during adsorption, the vapor flux through that pore is cut off and transport then depends on surface diffusion together with any bulk flow induced by the capillary forces. It is not generally recognized that the capillary suction is a contributor leading to the mass-transfer amplification (Weisz, 1975; Lee and Hwang, 1986; Abeles et al., 1991; Kärger and Ruthven, 1992; Radjy, 1974; Rajniak and Yang, 1996). Any capillary condensate volume elements will create a short-circuit effect leading to a reduction in the length of the diffusion path and a corresponding increase in the effective diffusivity. As a consequence, capillary condensation generally increases the total mass transport rate. As the relative pressure is increased, the number of pores that are still not filled with condensate decreases rapidly, and at point U, all pores are filled with capillary condensate. So, the first effect of the capillary condensation is to increase the mass transport rate when some pores are filled with condensate. For theoretical (infinite) media, the total mass transport rate during adsorption will increase in the capillary condensation region with an increasing number of pores being filled by capillary condensation, as shown in Figure 3b.

If the upper closure point U lies below $x = 1$, we can expect a decrease of the total mass transport rate for relative pressures $x^U < x < 1$, because in this region all pores are filled with capillary condensate and the transport is controlled by the flow of liquid condensate. For $x > x^U$, there exists a discontinuity in the concentration dependence of diffusivity that drops abruptly to the value characteristic of the system when the whole sample is filled with condensate. In this region, the transport is controlled by the liquid flow of capillary condensate during the compression of the condensate in the sample and flattening of the menisci. Such discontinuity is an artifact of the model for the theoretical infinite system of connected pores; and it does not exist in real systems. If the upper closure point U is at $x = 1$, capillary condensation accelerates the mass transport in the whole concentration range above point L. Theoretical prediction of diffusivity during adsorption is discussed in detail in our previous work (Rajniak and Yang, 1996).

The physical situation is quite different for the case of desorption or evaporation of the condensed adsorbate. While the condensation generally increases the mass transport rate, evaporation is a very slow process and one can expect a decrease in the total mass transport rate with an increasing role by evaporation from pores. For an infinite medium, there is no desorption between points U and T and diffusivity is zero in this region, as shown in Figure 3b. At the percolation threshold T, desorption starts and the diffusivity increases from zero. At point L, the two branches of concentration-dependent diffusivities coincide.

Theoretical models for infinite media successfully predict some qualitative features of the concentration dependence of diffusivity, that is, a rise in diffusivity during adsorption between points L and U and a rise in diffusivity between points T and L during desorption. However, the models cannot predict extremes on both dependencies, that is, a maximum for adsorption and a minimum for desorption, which are typical for the real finite systems.

One of the simplest methods for estimating the effective transport properties of disordered media is the effective medium approximation (EMA), which is a phenomenological method by which a disordered medium is replaced with a hypothetical homogeneous one represented by unknown

physical constants (Kirkpatrick, 1971; Sahimi, 1993). EMA thus transforms a many-body system into a one-body problem by which effective transport coefficients can be obtained.

The problem of mass transport in the porous adsorbent with randomly distributed fractions of pores filled by capillary condensation and by surface adsorption is similar to the problem of diffusion in a bi-disperse medium (Benzoni and Chang, 1984; Burganos and Sotirchos, 1987). Generally, a discrete multimodal distribution of pore diffusivities has the form

$$f(d) = \sum_{i=1}^{n} f_i \delta(d - d_i) \tag{8}$$

where δ is the Delta function and d_i is the diffusivity of the pore of the ith kind (such as, $d_i = d_s$ for the pore partially filled by surface adsorption and $d_i = d_c$ for the pore filled by capillary condensation) and n is the number of different fractions of pores. The EMA equation for the Bethe lattice with connectivity C (Stinchcombe, 1974; Heinrichs and Kumar, 1975; Sahimi, 1993) reduces to the summation

$$\sum_{i=1}^{n} f_i \frac{d_i - d_{\mathrm{EMA}}}{d_i + (C-2)d_{\mathrm{EMA}}} = 0 \tag{9}$$

where n is the number of different fractions of pores, d_{EMA} is the effective medium diffusivity, and d_i is the diffusivity of the pore of type i.

The value of d_{EMA} computed from the effective medium equation (Eq. 9) is related to the effective diffusivity of the whole network D_{EMA} (Stinchcombe, 1974) by

$$D_{\mathrm{EMA}} = C\frac{(C-2)}{(C-1)} d_{\mathrm{EMA}} \tag{10}$$

The following assumptions are made for all ensuing models:

(1) For relative pressures $x < x^L$, all pores of the porous medium are partially filled by surface adsorption, while for $x > x^U$ all pores are filled by capillary condensation. For $x^L < x < x^U$, that is, in the hysteresis domain, the pores are partially filled by surface adsorption as well as capillary condensation.

(2) The fraction of pores filled by capillary condensation is S and that by surface adsorption is $1 - S$. For primary adsorption S_A is given by Eq. 4 and for primary desorption S_D is given by Eqs. 5 and 6.

(3) The symbol d_S was used for the diffusivity in the pore site that is partially filled by surface adsorption and d_C for the diffusivity in the pore site that is filled by capillary condensation during adsorption in the hysteresis region. (Mass transport occurs in pores containing condensate by pressure-driven flow, rather than diffusion, and the use of d_C is a formal simplification.) Similarly, we will use the symbol d_E for the diffusivity in the pore site that is filled by capillary condensation during desorption in the hysteresis region. We will use the symbol d_F for the diffusivity in the pore site that is filled by capillary condensation in the region of flow of capillary condensate, that is, for relative pressures $x > x^U$.

(4) We will assume $d_E < d_S < d_C$ (that is, evaporation is slower than surface adsorption which is slower than capillary condensation), and also $d_F < d_C$ (that is, flow of capillary condensate is slower than diffusion of capillary condensate).

(5) The bonds (pore throats and windows) between the pore sites do not contribute significantly to the total volume and the volume of capillary condensed liquid is associated only with the pore sites.

Based on the foregoing discussion, the model for the adsorption kinetics in the infinite media is given by Model A1 as follows:

Model A1:

For $x \le x^L$:

$$f_1 = 1 \quad f_2 = 0 \qquad d_{\mathrm{EMA}} = d_S$$

For $x^L < x < x^U$:

$$f_1 = 1 - S_A \qquad f_2 = S_A \qquad d_1 = d_S \qquad d_2 = d_C$$

d_{EMA} given by solution of Eq. 9 for $n = 2$

For $x \ge x^U$:

$$f_1 = 0 \quad f_2 = 1 \quad d_{\mathrm{EMA}} = d_F$$

The dependence of the effective diffusivity for Model A1 is shown in Figure 3b. Model A1 is equivalent to Model 2 discussed in our previous article (Rajniak and Yang, 1996), where the theoretical dependencies for various values of connectivity are also shown. The dependence of diffusivity contains a maximum at $x = x^U$. For $x > x^U$, there exists a discontinuity in the concentration dependence of diffusivity that decreases abruptly to the value d_F.

The model for desorption kinetics in the infinite media that is discussed in the present analysis (Model D1) is summarized as follows:

Model D1:

For $x \ge x^U$:

$$f_1 = 0 \qquad f_2 = 1 \qquad d_{\mathrm{EMA}} = d_F$$

For $x^T < x < x^U$:

$$f_1 = 0 \qquad f_2 = S_D = 1 \qquad d_{\mathrm{EMA}} = 0$$

For $x^L < x < x^T$:

$$f_1 = 1 - S_D \qquad f_2 = S_D \qquad d_1 = d_S \qquad d_2 = d_E$$

d_{EMA} given by solution of Eq. 9 for $n = 2$

For $x \le x^L$:

$$f_1 = 1 \qquad f_2 = 0 \qquad d_{\mathrm{EMA}} = d_S$$

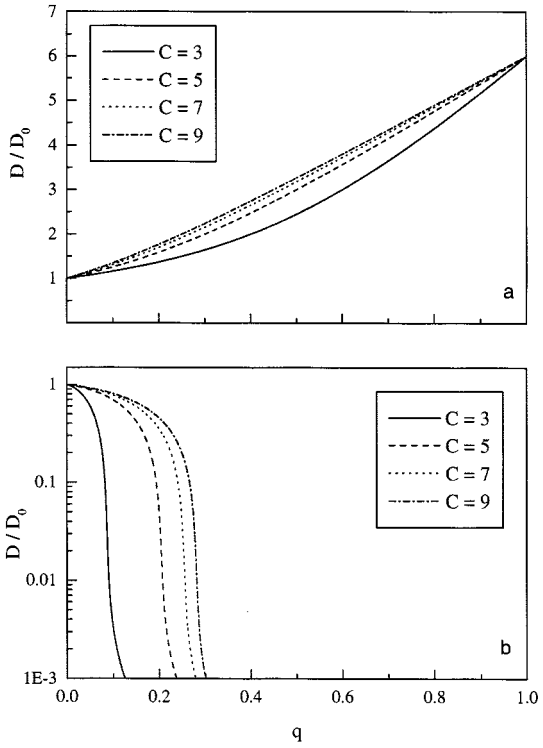

Figure 4. Theoretical dependencies of diffusivity on pore-filling (q) for various connectivity (C).

For (a) adsorption (Model A1); (b) desorption (Model D1).

The theoretical dependence of the effective diffusivity based on Model D1 is shown in Figure 3b. The model predicts a decreasing diffusivity between points L and T, which is observed also for real systems. Between points T and U, the diffusivity is zero indicating no desorption or mass transfer in this region.

In Figure 4 the theoretical dependencies of effective diffusivity for various connectivities are shown for both adsorption and desorption. Models A1 and D1 successfully predict the basic features of experimental results, that is, a maximum in diffusivity during adsorption and a minimum during desorption. However, there exist artifacts in the models which need further discussion, that is, discontinuity in the concentration dependence during adsorption and zero diffusivity in the concentration dependence during desorption.

Adsorption-desorption equilibria for finite systems

From the viewpoint of the equilibrium behavior, the primary adsorption process in the capillary condensation region can be treated as a classic site percolation problem. The pore sites of the network are filled by capillary condensate with probability q and partially filled by surface adsorption with probability $1-q$. As discussed earlier, whether a particular site is filled by capillary condensation depends only on its characteristic dimension, while the connectivity of the pores is irrelevant, and the primary adsorption for the real systems, that is, porous media with finite dimensions, is the same as that for the infinite systems described by Eqs. 2, 3a, and 4.

Disagreement between theory and experiment exists for the case of real primary desorption, since the real desorption

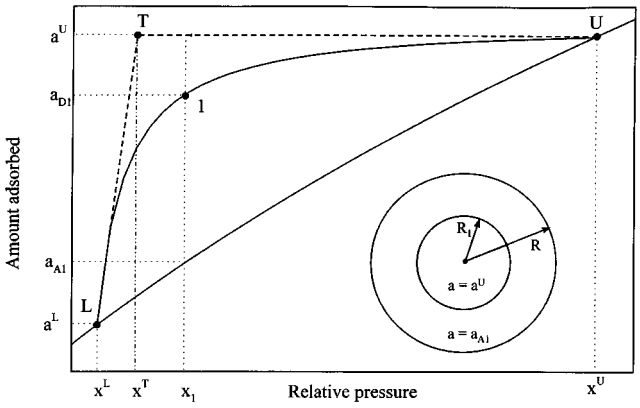

Figure 5. Desorption equilibria for finite systems.

Amount adsorbed in the shell a_{A1} and in the core a^U at point 1 on the experimental primary desorption curve where the amount adsorbed is a_{D1} (inset) shell and core of the microparticle for amount adsorbed a_{D1} (see also Eq. 11).

isotherm is not horizontal and desorption does occur. Various explanations for this fact were discussed in our previous work (Rajniak and Yang, 1994) and empirical correction functions were proposed for computation of the real amount adsorbed during primary desorption, as well as during higher-order desorption processes. However, most of the theoretical and experimental studies indicate that the finite size of the microparticles of the porous material and corresponding desorption from the surface of the microparticles is the most important reason of the disagreement. The real primary desorption can be described by various relations (Rajniak and Yang, 1993, 1994). However, use of either Langmuir or Dubinin or other kind of adsorption equilibria relationship for the hysteresis-dependent desorption is only a mathematical simplification.

Some properties of the Bethe trees make them unsuitable for evaluating surface effects of the real media. The fraction of the sites of the Bethe tree that are on its surface is given by $(C-2)/(C-1)$. This means that, in a Bethe lattice, most of the sites (or bonds) are on the surface, whereas, in reality, this fraction is small. So the Bethe tree model of the pore structure can be used only for the core of the microparticle and another approach has to be used for the surface.

In this work, a new approach based on mass balance of the adsorbed material in the particle will be used to evaluate the amount adsorbed during primary desorption. We assume that between points T and U in Figure 5, as the pressure decreases, the condensed adsorbate is able to vaporize only from some pores near the outer surface of the microparticle, and then from some of the pores adjacent to those vapor filled pores, so that clusters of vapor filled pores (or surface clusters) grow on the outer surface of the microparticle. The vapor phase increasingly penetrates the surface layer of the microparticle. At the same time, the bonds in the bulk of the microparticle form clusters of bonds in which the adsorbate is below its condensation pressure but without access to the vapor phase. Only at the percolation threshold, the bonds in the bulk of the microparticle form a percolating cluster that has access to the outer surface, and desorption from the bulk of the microparticle can start. The decrease in the amount

adsorbed between points U and T on the real primary desorption isotherm is a consequence of the desorption from the surface cluster of the microparticle of the porous material. Next we assume that there is a distinct boundary between the surface shell (that is partially desorbed) and the bulk core (that is completely filled) for the microparticle (see Figure 5 inset). At relative pressure x ($x^T < x < x^U$), the core is completely filled with liquid condensate, that is, the fraction of the pores filled in the core is $S = 1$ and the amount adsorbed is a^U, while the fraction of pores filled in the shell is equal to S_A, the fraction corresponding to the primary adsorption isotherm (that is, the amount adsorbed is a_A). The mean value of the fraction filled in the whole microparticle is obviously S_D, the fraction corresponding to the real primary desorption isotherm (the amount adsorbed is a_D). From the material balance on the microparticle, it is then easy to evaluate the thickness of the core R_1

$$R_1 = R\sqrt[3]{\frac{a_D - a_A}{a^U - a_A}} = R\sqrt[3]{\frac{S_D - S_A}{1 - S_A}} \tag{11}$$

The material balance (Eq. 11) and the evaluation of the core and shell thicknesses are important also for the desorption kinetics prediction for real finite systems.

Adsorption-desorption kinetics for finite systems

The theoretical relations of Model A1 were developed for the idealized case of an infinite network (that is, Bethe tree), in which all pores are conductive. There are neither blind pores nor nonconductive pores, and the effect of decreasing the total mass transport rate by the influence of the flow of capillary condensate in pores completely filled by the condensate is important only for $x \geq x^U$. In real porous adsorbents, there exists both blind (dead-end) pores and nonconductive pores.

The problem of nonconductive pores was discussed by Radjy (1974) and Lee and Hwang (1986). They assumed that in a cylindrical pore, an annular film is formed on the solid wall and considered that the thickness of this film is the same as the thickness of the adsorbed layer on a free surface not subject to capillary condensation. Therefore, it increases when the vapor concentration increases and the smallest pores may become completely nonconductive at higher relative pressures. The fraction of pores that are nonconductive will increase with increasing pressure as well as with increasing q.

The blind (dead-end) pores are accessible for filling by surface adsorption and capillary condensation; but, after filling with capillary condensation, they do not increase the total mass transport rate, but on the contrary, decrease it, because they do not conduct the flow. Again, the fraction of pores that belongs to the blind clusters will increase with increasing q. For $q = 1$, all pores are filled with condensate and belong to blind clusters. Therefore, in real porous adsorbents with a broad pore-size distribution and with the presence of the blind pores, all three main mechanisms (surface diffusion, capillary condensation, and liquid flow of capillary condensate) may already be operative simultaneously below point U. The existence of nonconductive or blind pores can explain the maximum in the concentration dependence of diffusivity during adsorption at a relative pressure $x < x^U$. In our previous work (Rajniak and Yang, 1996), a model was proposed by taking into account the empirical fraction of blind pores. Using that previous model with an adjustable quantity a^*, it was possible to fit the experimental diffusivity data. A similar approach can be used to take into account also the existence of the nonconductive pores.

In this work we formulate a completely predictive approach based on the properties of Bethe trees. For such lattices, the analytical solution for the evaluation of the fraction of liquid filled pores without connection to infinity (exterior surface) B is available (Stinchcombe, 1974; Larson and Davis, 1982), that is,

$$\sum_{j=2}^{C-1} B^{C-j} + \frac{q-1}{q} = 0 \tag{12}$$

and

$$Q = 1 - B \tag{13}$$

represents the probability that an arbitrarily chosen conducting branch leaving a given site is an infinite cluster.

We will define a ''blind'' liquid-filled pore as one having also all its C neighbors liquid filled and with all its C neighbors connected to infinity (external surface) via at least one connected pathway of liquid-filled pores. The situation is shown in Figure 6. So the probability s that any pore is ''blind'' is given by probability q (that a given pore is liquid filled) multiplied by q^C (the probability that all its C neighbors are also liquid filled) and multiplied by probability Q^C (that all C neighbors have at least one liquid-filled branch connected to infinity), that is,

$$s = qq^C Q^C \tag{14}$$

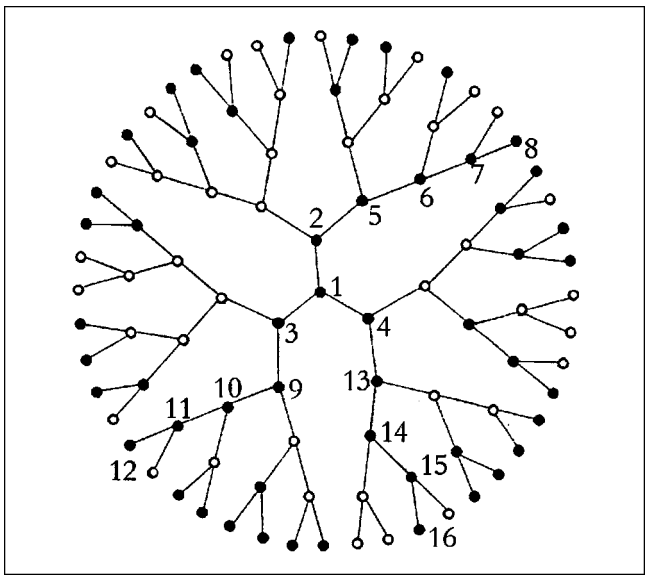

Figure 6. Dead-end (blind) pore for Bethe tree network.

The filled central pore is blind because all three neighbors (pores 2, 3, 4) are filled and connected to infinity (surface) via at least one connected pathway of liquid-filled pores (that is, pathway 2-5-6-7-8, pathway 3-9-10-11-12, and pathway 4-13-14-15-16).

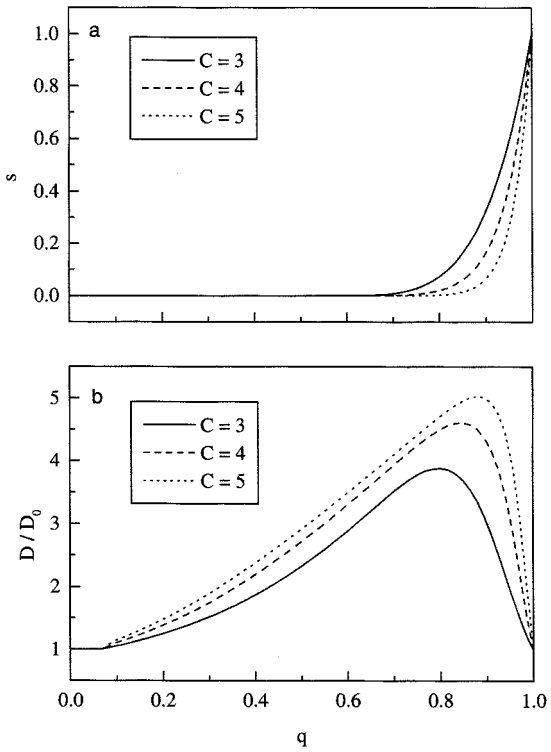

Figure 7. Adsorption kinetics for finite systems vs. fraction of pores filled.

(a) Fraction of blind pores (s) for various connectivity (C) (Eqs. 12–14); (b) dependence of diffusivity for various connectivity $d_S = d_F = 1$, $d_C = 6$.

The theoretical dependence of the fraction of blind pores s as a function of q is shown in Figure 7 for various values of connectivity.

The model for the adsorption kinetics for the finite (real) media incorporating the existence of the blind pores is therefore given below:

Model A2:

For $x \le x^L$:

$$f_1 = 1 \qquad f_2 = f_3 = 0 \qquad d_{\mathrm{EMA}} = d_S$$

For $x^L < x < x^U$:

$$f_1 = 1 - q \qquad f_2 = q(1 - s) \qquad f_3 = qs$$

$$d_1 = d_S \qquad d_2 = d_C \qquad d_3 = d_F$$

s given by solution of Eqs. 12–14

d_{EMA} given by solution of Eq. 9 for $n = 3$

For $x \ge x^U$:

$$f_1 = f_2 = 0 \qquad f_3 = 1 \qquad d_{\mathrm{EMA}} = d_F$$

The theoretical dependence of the effective diffusivity based on Model A2 for various values of connectivity is shown in Figure 7b as a function of pores filled by capillary condensation q. Comparing Figures 7a and 7b, it can be concluded that the acceleration of the mass transport rate is more pronounced for higher values of connectivity where the existence of blind pores is less important. A higher value of connectivity also shifts the position of the maximum diffusivity to a higher value of concentration.

The use of EMA employed in the development of the network model for mass transfer during adsorption is based on the assumption that the various classes of pore diffusivities (conductances) are spatially distributed at random. This assumption is valid for the case of adsorption, because all the pores accessible to a given phase are effectively occupied by it. Its validity is more doubtful for desorption when the spatial topology of the phases is influenced by pore blocking. As a consequence of pore blocking for the infinite systems, there is no desorption and no mass transport for concentrations higher than that corresponding to the percolation threshold. This problem was already discussed above, and, for real finite systems, it seems to be logical that the desorption begins for the higher concentrations when evaporation proceeds from the external surface of the finite microparticle. In the second step the boundary of the phase separation along the widest pores connected with the external surface penetrates into the pellet (microparticle) volume.

For desorption kinetics for the real finite system, the following assumptions are made:

(1) There exist two basic configurations inside the microparticles of the adsorbent, that is, a completely filled core and a partially filled shell. The thickness of the core R_1 is given by Eq. 11 (see also Figure 4).

(2) For mass transport in the core, the model for infinite medium (Model D1) can be used, that is, there is no desorption from the core for $x > x^T$.

(3) There is no pore blocking (and no hysteresis) in the shell, and mass transport in the shell occurs at all relative pressures.

Following the discussion above, the model for predicting the effective diffusivity for desorption in the finite media is summarized as follows:

Model D2:

For the whole particle:

For $x \ge x^U$:

$$f_1 = 0 \qquad f_2 = 1 \qquad d_{\mathrm{EMA}} = d_F$$

For $x \le x^L$:

$$f_1 = 1 \qquad f_2 = 0 \qquad d_{\mathrm{EMA}} = d_S$$

For the core:

For $x^T < x < x^U$:

$$f_1 = 0 \qquad f_2 = S_D = 1 \qquad d_{\mathrm{EMA,core}} = 0$$

For $x^L < x < x^T$:

$$f_1 = 1 - S_D \qquad f_2 = S_D \qquad d_1 = d_S \qquad d_2 = d_E$$

$d_{\mathrm{EMA,core}}$ given by solution of Eq. 9 for $n = 2$

For the shell:
For $x^L < x < x^U$:

$$f_1 = 1 - S_A \qquad f_2 = S_A \qquad d_1 = d_S \qquad d_2 = d_E$$

$$d_{\mathrm{EMA,shell}} \text{ given by solution of Eq. 9 for } n = 2$$

The theoretical dependence of the effective diffusivity for both core and shell is shown in Figure 8. The dependence fore the core diffusivity is the same as that by Model D1 (see Figure 3b). Both diffusivities decrease with an increasing relative pressure, and they join at the two limiting points of the main hysteresis loop L and U. However, there is no minimum in any of the dependencies.

From adsorption-desorption experiments (such as by a gravimetric method), we can evaluate only one apparent diffusivity which is representative of the whole microparticle. In the next part, the models of diffusion in the finite microparticle are formulated for both adsorption and desorption. Theoretical prediction of the apparent diffusivity is also discussed in the following.

Models for mass transport in a single microparticle

Processes in porous media can be studied by the continuum approach or the discrete approach. The present study refers to the discrete approach and is based on a representation of the pore space as a network of interconnected pores.

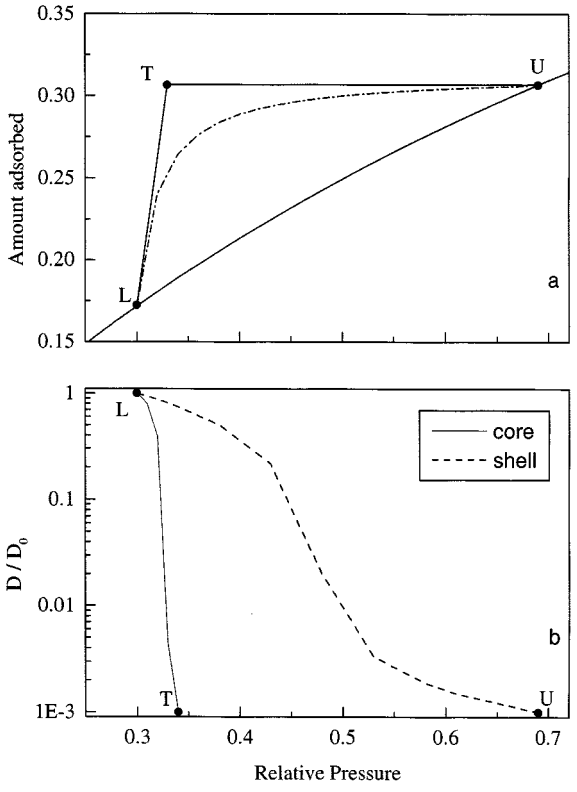

Figure 8. Theoretical prediction of diffusivities by Model D2 for system silica gel-water.

(a) Equilibria and (b) diffusivity for shell D_{shell} and core D_{core} computed using Model D2 with $d_S = 1$ and $d_E = 0.001$.

The effective medium approximation is then used for evaluation of the effective diffusivities of the disordered medium. Then, the continuum model based on the diffusion equation (Fick's law) can be employed. From the foregoing analysis, it is clear that effective diffusivities for adsorption and desorption are strongly concentration-dependent. However, if the uptake occurs over a small step change in the adsorbed-phase concentration, and with sufficiently high total flow rate, we may assume the absence of external heat- and mass-transfer resistances. We also assume isothermal behavior during the sorption. Then, the mass transport in a spherical microparticle with radius R can be represented by the transient diffusion equation with a constant diffusivity:

Model A3

$$t < 0 \qquad 0 \le r \le R \qquad a = a^0 \tag{15}$$

$$t \ge 0 \qquad r = R \qquad a = a_\infty \tag{16}$$

$$r = 0 \qquad \frac{\partial a}{\partial r} = 0 \tag{17}$$

$$0 < r < R \qquad \frac{\partial a}{\partial t} = D\left(\frac{\partial^2 a}{\partial r^2} + \frac{2}{r}\frac{\partial a}{\partial r}\right) \tag{18}$$

The analytical or numerical solution of Eqs. 15–18 is available (Kärger and Ruthven, 1992; Rajniak, 1985). For predictions of mass transport in the particle during adsorption, the mathematical model A3 can be used with $D = D_{\mathrm{EMA}}$ computed via Model A2 and Eq. 10.

This model can also be used for desorption assuming constant diffusivity in the whole microparticle. However, the prediction of mass transport during desorption is more complicated. As discussed earlier, there are various configurations of pores and, consequently, various ''diffusivities'' in the core and in the shell. The mathematical model then contains transient diffusion equations for the core and for the shell.

Model D3

$$t < 0 \qquad 0 \le r < R_1 \qquad a = a^0_{\mathrm{core}} \tag{19}$$

$$R_1 \le r \le R \qquad a = a^0_{\mathrm{shell}} \tag{20}$$

$$t \ge 0 \qquad r = R \qquad a = a_\alpha \tag{21}$$

$$r = R_1 \qquad D_{\mathrm{EMA,core}}\left(\frac{\partial a}{\partial r}\right)_- = D_{\mathrm{EMA,shell}}\left(\frac{\partial a}{\partial r}\right)_+ \tag{22}$$

$$r = 0 \qquad \frac{\partial a}{\partial r} = 0 \tag{23}$$

$$0 < r < R_1 \qquad \frac{\partial a}{\partial t} = D_{\mathrm{EMA,core}}\left(\frac{\partial^2 a}{\partial r^2} + \frac{2}{r}\frac{\partial a}{\partial r}\right) \tag{24}$$

$$R_1 < r < R \qquad \frac{\partial a}{\partial t} = D_{\mathrm{EMA,shell}}\left(\frac{\partial^2 a}{\partial r^2} + \frac{2}{r}\frac{\partial a}{\partial r}\right) \tag{25}$$

Core and shell diffusivities are predicted by Model D2 and Eq. 10. The numerical solution of Eqs. 19–25 is done using a global spline orthogonal collocation method (Villadsen, Michelsen, 1978; Rajniak, 1985). Finally, the apparent Fickian diffusivity D_{app} for the whole particle is obtained by matching the solution of the Model A3 with $D = D_{app}$ to the solution of Model D3.

Experimental Studies

Vycor glass and silica gel were used in the experiments. Vycor is a porous glass which has been widely used as a model material in studies of properties of fluids and molecules in highly confined geometries. The large internal surface area of Vycor effectively adsorbs molecules at low ambient vapor pressures, while the large pore volume effectively absorbs bulk fluids by capillary condensation at higher ambient vapor pressures (Page et al., 1993). Silica gel, Davison Grade H, a standard commercial desiccant was used in our previous experiments (Rajniak and Yang, 1993, 1994, 1996).

Sorption data for nitrogen at liquid nitrogen temperature 77 K were obtained using a Carlo Erba Sorptomatic 1900 apparatus for both sorbents. The Sorptomatic 1900 is a fully automatic instrument for measuring the adsorption and desorption of gases (usually nitrogen) on a solid sample. It uses a multipoint technique for determining the complete adsorption and desorption isotherms from which specific surface area (using either B.E.T. or the Dubinin equation according to the sample), and pore-size/pore-volume distributions of solids are obtained. A complete adsorption-desorption isotherm, which usually takes hours of operation, is obtained automatically.

Equilibrium results for the system silica gel-nitrogen have shown complete reversibility through the entire pressure range. On the other hand, results for the system Vycor glass-nitrogen have shown a significant hysteresis loop. The specific BET surface area and pore volume for the silica gel were determined to be 767 m^2/g and 0.398 cm^3/g, respectively. The BET surface area and pore volume for the Vycor glass were 189 m^2/g and 0.715 cm^3/g, respectively.

For the system silica gel-water vapor, the equilibrium and the kinetic data were measured using a Mettler TA2000C Thermoanalyzer (TGA). For the kinetic data measurement, the flow conditions were adjusted to avoid or minimize influence by external diffusion. The total flow rate of the mixture flowing to the TGA was measured by using two additional gas wash bottles. The experimental conditions were adjusted to ensure that the external diffusion resistance was absent (or minimized to a negligible level) and that the wet helium stream was indeed saturated (Rajniak and Yang, 1996). The equilibrium and kinetic data for the system Vycor glass-nitrogen were measured using the Sorptomatic 1900 described above. There was no influence by external diffusion, because pure nitrogen was used in the experiments.

In the diffusivity measurement, the sample initially at equilibrium was subject to a sudden small change in partial pressure and the weight changes during adsorption or desorption were continually recorded. The heat effects during the sorption measurements were minimized by allowing only small step changes in relative pressure during each measurement. Because the sorption rates were independent of the pellet size, we can assume that the total sorption rate was controlled by the mass transport processes within the microparticles. Successive adsorption and desorption were conducted by changing the composition of the adsorptive and allowing adequate time to establish equilibrium.

Results and Discussion

In all figures the experimental and theoretical diffusivity data are normalized. The data are ratioed against the Fickian diffusivity at the lower closure point of the hysteresis loop D_o. The ratio D/D_o is plotted in all figures. The mass transport process is expected to be reversible in the region of surface diffusion. Study of the concentration dependence of diffusivity below the lower limiting point L and above the upper limiting point U is out of the scope of this work. Evaluation of the absolute values of the diffusivities for the systems studied in this work requires information on the characteristic dimension of the microparticle in which the mass transport process occurs. The term diffusivity is also used in the formulation of the EMA model for pores of various kinds, such as for pores in which only surface diffusion occurs and for pores in which capillary condensation occurs.

The experimental rate data for adsorption are first analyzed. The data for the system silica gel-water vapor reported earlier (Rajniak and Yang, 1996) are treated with the improved network model for adsorption kinetics Model A2. The experimental results at 298 K are compared in Figure 9 with the predictions from the models A1 and A2. The experimental concentration dependence of the diffusivity shows a maximum near the upper closure point U. In comparison to the results of Model A1 for an infinite medium presented earlier (Rajniak and Yang, 1996), a significant improvement in the theoretical prediction is seen. The prediction by Model A2 is based completely on theoretical considerations. The value of the connectivity $C = 3$ was evaluated from the equilibrium data using Mason's method (Mason, 1988; Rajniak and Yang,

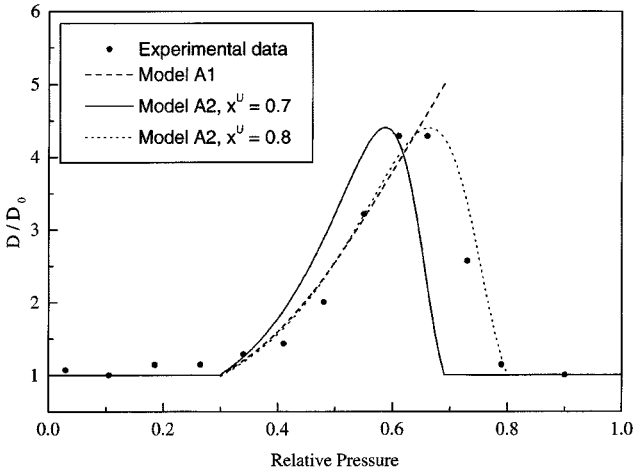

Figure 9. Experimental diffusivity vs. theoretical predictions by Models A1 and A2 for the system silica gel-water vapor at 298 K for the adsorption case.

$d_S = 1$, $d_C = 5$.

1996). All the other parameters used for the theoretical prediction are the same as reported earlier, that is, positions of the limiting points of the main hysteresis loop and parameters of the primary adsorption isotherm. The only adjustable parameter for the diffusivity prediction by Model A2 is the ratio of the diffusivity in the capillary condensation region and that of the surface diffusivity, that is, d_c/d_s. No adjustable parameters similar to x^* (the empirical relative pressure at which the blind pores become filled with capillary condensate (Rajniak and Yang, 1996) are needed here.

The analytical relations (Eqs. 12–14) for the evaluation of the fraction of ''blind'' pores are derived using the Bethe tree lattice as the model for the pore network. This is the main advantage of the Bethe lattice, as it is often possible to derive analytical formulas for the properties of interest; and often the predictions of such formulas agree surprisingly well with those of three-dimensional systems (Sahimi, 1995). As discussed also by Mason (1988), general forms of the percolation properties that are known for both crystal structures and Bethe trees show surprising similarities.

The use of EMA in the development of the network model for mass transfer during adsorption is based on the assumption that the various classes of pore diffusivities (conductances) are spatially distributed at random. This assumption is valid for the case of adsorption, because all the pores accessible to a given phase are effectively occupied by it. The approach derived here solves the main artifact of our earlier model (Rajniak and Yang, 1996), that is, a discontinuity in the concentration dependence of diffusivity.

Model A2 represents the next step in the unification of the equilibrium theory based on the pore-blocking interpretation of hysteresis and the percolation model of mass transport in the network of pores randomly filled by capillary condensate or surface adsorption. Using Model A3, the mass transport process in the particle can be predicted using diffusivity values calculated from Model A2.

The main objective of the present work is to develop and check the validity of the network model for the difficult problem of desorption kinetics, which has not been done previously. Experimental kinetic data available in the literature for the capillary condensation regime (Rhim and Hwang, 1975; Tamon et al., 1981; Toei et al., 1983; Eberly and Vosberg, 1965) cannot be compared with predictions from our models because either the equilibrium data are incomplete, are missing, or the kinetics data are for the adsorption case only. Therefore, it was necessary to measure new sets of complete equilibrium and kinetic data. Two systems, silica gel-water vapor and Vycor glass-nitrogen, were studied. The complete equilibrium data for the system silica gel-water vapor were published elsewhere (Rajniak and Yang, 1993, 1994). The kinetic data for adsorption are analyzed above (see Figure 9).

In Figure 10 the experimental data of the relative Fickian diffusivity for desorption for the system silica gel-water vapor are shown and are compared to the theoretical predictions. The experimental concentration dependence of the diffusivity shows a minimum near the lower closure point L. Using the equilibrium data and following the theory presented in the foregoing, Model D2 is used to predict diffusivities in the core and in the shell. Model D3 uses predictions from Model D2 for calculating the core and shell diffusivities and subsequently yields the overall diffusivity for the whole particle. Starting from the concentration (or relative pressure) $x = x^U$ and decreasing relative pressure by small changes, we solve Model D3 for $D_{\mathrm{EMA,core}}$ and $D_{\mathrm{EMA,shell}}$ that are predicted by Model D2. By matching the solution of Model D3 to the solution of the diffusion equation (Model A3 is for the desorption case), we obtain the overall value D for each transient. The results are normalized by dividing by the diffusivity D_o.

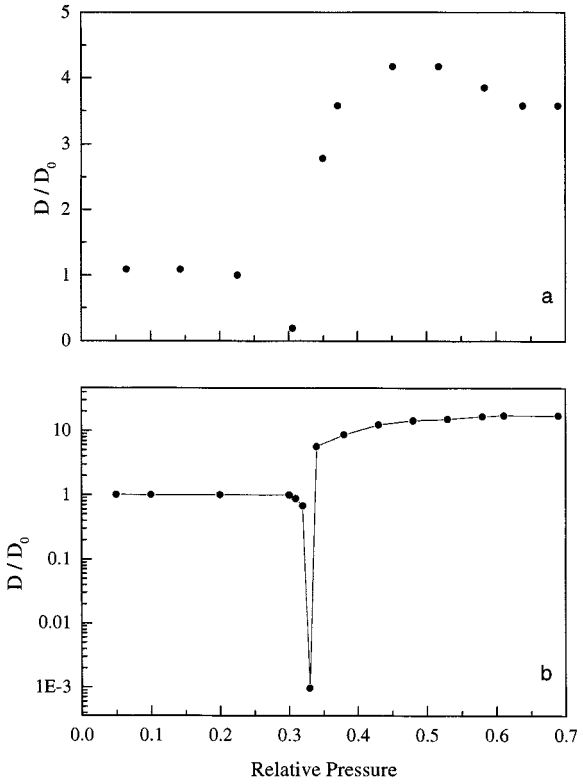

Figure 10. Experimental diffusivity data (a) vs. theoretical predictions (b) by using Model D3 for the system silica gel-water vapor at 298 K, for the desorption case.

$d_S = 1$; $d_E = 0.001$.

For relative pressures $x > x^T$, desorption (evaporation) occurs only from this shell at the microparticle surface. The thickness of the shell increases with decreasing x. Both diffusivities D_{core} (for the completely saturated core) and D_{shell} (for the partially saturated shell) increase with decreasing pressure (see Figure 8b), but the overall diffusivity D for the whole particle decreases in this region. This is because desorption proceeds in an increasingly thicker shell (with thickness R_1 given by Eq. 11), and the corresponding diffusion path increases. It is seen that the increasing diffusion path dominates over the accelerating effect of the shell and core diffusivities. When the concentration is dropped below x^T, desorption starts also from the core and the diffusivity passes through a minimum, as shown in Figure 10. The mass transport (desorption) is very slow in this region and an unusual transient behavior occurs. In this stage the process is very slow, first, because desorption (evaporation) occurs from the whole core, that is, the mass-transfer path for the core molecules is the longest, and secondly, because the evapora-

tion (which is slow process alone) occurs from the maximum amount of pores and in the pore space with the minimum number of empty pores. (Also, the mass-transfer path in the core alone is the longest and curved, because of only few empty pores, that is, high tortuosity.) For relative pressures smaller than threshold relative pressure, the desorption (evaporation) occurs already from the whole microparticle. There is still pore blocking, but the fraction of empty (non-blocking pores) is increasing with decreasing pressure, that is, the apparent diffusivity is increasing. This branch is nicely predicted from the theoretical relations for infinite medium (no surface effects), as shown in Figure 3b.

The theoretical and experimental results are in qualitative agreement. The theoretical model successfully predicts the position of the minimum in diffusivity between points T and L. The model also predicts higher values for the overall, apparent diffusivity in the concentration range between points U and T, compared to the diffusivities between points T and L. However, quantitative agreement is not satisfactory. The maximum experimental relative diffusivity is 4.2 and the minimum experimental diffusivity is 0.19, while the theoretical maximum relative diffusivity is 17.4 and the minimum is 0.001.

In Figure 11 typical dependencies of the amount adsorbed during desorption for the system silica gel-water are compared for concentrations higher and lower than the percolation threshold x^T. The desorption (evaporation) process at the percolation threshold (close to the lower limiting point L) is unusually slow. Also, the shape of the transient amount adsorbed at this point (for the relative pressure change from 0.35 to 0.306) is different from the Fickian behavior observed at other concentrations. The mass transport at this point involves a combination of various mechanisms (surface diffusion, evaporation, condensation, and liquid flow), and modeling the mass transport process by the diffusion equation is an oversimplification.

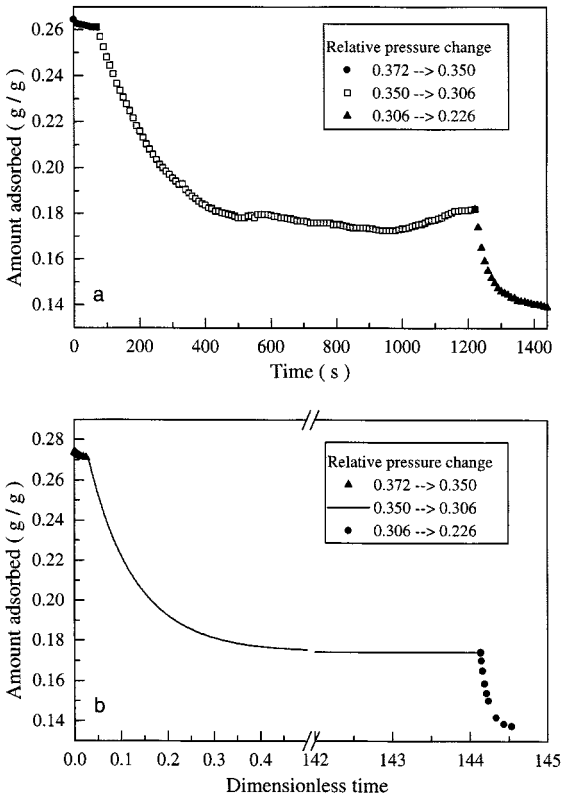

Figure 11. Desorption upon step changes in relative pressure for the system silica gel-water at 298 K.

(a) Experimental; (b) predictions by Model D3.

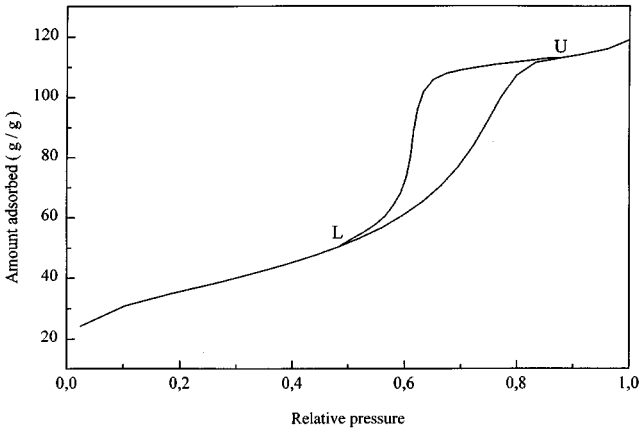

Figure 12. Experimental adsorption-desorption equilibrium data for the system Vycor glass-nitrogen at 77 K.

Figure 12 shows the experimental data for adsorption-desorption equilibria for the system Vycor glass-nitrogen at 77 K. The primary adsorption isotherm of type IV and the primary desorption isotherm of type H2 are observed.

In Figure 13 the experimental data of the relative Fickian diffusivity for desorption for the system Vycor glass-nitrogen are shown and are compared with the theoretical predictions. The behavior of the system is qualitatively similar to that of silica gel-water, that is, with a decreasing diffusivity going from point U to point T, passing through a minimum near the threshold point T, followed by an increasing diffusivity between points T and L. Compared with the results for the system silica gel-water, it was possible to measure more experiments data points between points T and L.

The theoretical model is again able to predict well, qualitatively, the concentration dependence of the diffusivity, but the quantitative agreement is understandably poor. The maximum experimental relative diffusivity is 1.92 and the minimum experimental diffusivity is 0.13, while the theoretical maximum relative diffusivity is 18.34 and the minimum is 0.046.

There are several possible reasons for the quantitative discrepancy between the theory and experiment for the case of desorption kinetics:

(1) The boundary between the shell and the core is assumed to be distinct in the theoretical model, as shown in Figure 5. In the real microparticle the boundary is a diffuse one. An improved model with a third (middle) zone between the core and the shell should better describe the reality. The mass transport path will be longer for molecules from the middle zone. As a consequence, the apparent diffusivity will be smaller for the descending branch of the diffusivity dependence. Another consequence will be an acceleration of

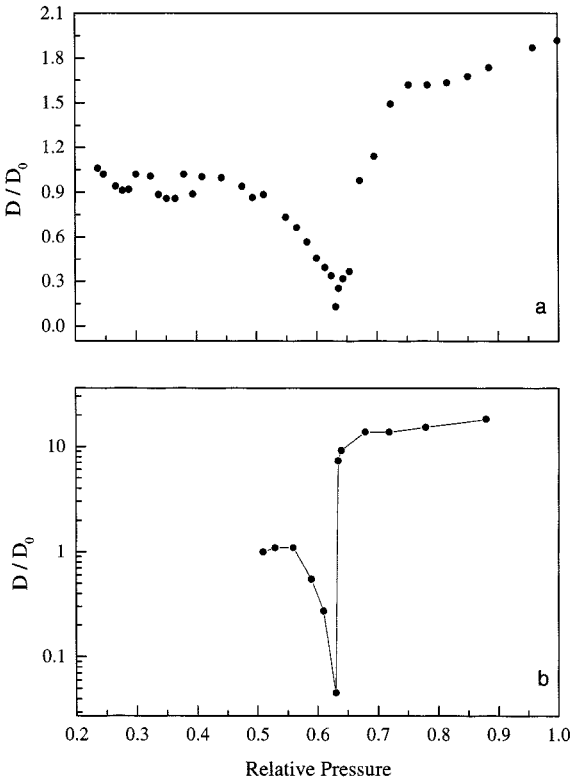

Figure 13. Experimental desorption diffusivity data.

(a) Vs. theoretical predictions; (b) by using Model D3 for the system Vycor glass-nitrogen at 77 K. $d_S = 1$, $d_E = 0.001$.

the process for relative pressure $x \leq x^T$, because slow evaporation will occur from the smaller core. So, the addition of the middle zone should decrease the maximum and increase the minimum of the theoretical dependence of diffusivity without changing the correct position of the minimum.

(2) The use of EMA in the development of the network model for mass transfer in the shell assumed that various classes of pore diffusivities (conductances) are randomly distributed in the shell. This assumption is valid for the case of adsorption, because all the pores accessible to a given phase are effectively occupied by it. It is less so for desorption. The spatial topology of the phases is influenced by pore blocking, and the distribution of phases is not random, especially in the shell for concentrations higher than the percolation threshold.

(3) The model assumes only surface diffusion and evaporation during desorption in the hysteresis region and is thus much simplified. From the theoretical and experimental study of Abeles et al. (1991), different flow regimes can exist depending on the magnitude of the vapor and/or liquid pressures at the inlet and outlet sides of the porous medium. Results of Laurindo and Prat (1996) indicate that film flows could be important in evaporation and, more generally, in phase change phenomena in porous media. Other possible complicating effects are nucleation (Parlar and Yortsos, 1989), decompression of the condensed liquid (Mason, 1988), and flow of conductance by gravity (Prat, 1995).

(4) Simultaneous evaporation and condensation processes during the emptying of the pores of various dimensions combined with the actual nonisothermality can slow down the process.

(5) There exist possible loops in the path of mass transport during desorption, because of nonrandom distribution of phases. It is known that if a particular percolation property depends on the existence of loops, then the use of the Bethe tree would not be appropriate.

(6) The assumption that the diffusivities (or conductances) of the pores of various dimensions are constant could be an oversimplification.

The study of equilibria and kinetics for adsorption-desorption systems with hysteresis shows that the concepts of percolation theory play a prominant role. Theoretical predictions are excellent for simpler percolation processes, that is, desorption equilibria (bond percolation) and adsorption kinetics (ordinary percolation). Qualitative agreement is also obtained for desorption kinetics (invasion percolation), but quantitative agreement is not satisfactory for this complicated process of the invasion percolation type. For such processes, further studies are needed. Numerical Monte Carlo simulation of the percolation processes on a more realistic (but more complex) pore network, such as the diluted simple-cubic lattice, should improve the agreement between model and experiment. However, for engineering purposes (such as within a process simulation), it is always useful to have a quick solution that is capable of predicting limiting behaviors of the process, as given in this contribution.

Conclusion

Network models are formulated for predicting the concentration dependence of the Fickian diffusivity for systems exhibiting hysteresis in adsorption-desorption equilibria.

Adsorption-desorption equilibria and kinetics are studied both experimentally and theoretically. The main results are as follows:

(1) For adsorption, the network model of mass transport of condensable vapors in porous media based on the combination of the percolation model of mass transport in the pore network with the effective medium approximation (Rajniak and Yang, 1996) is further improved. A new predictive relation based on the properties of Bethe lattices is proposed to account for the existence of liquid-filled "blind" pores that decrease the total mass transport rate.

(2) For desorption, a new "shell and core" (or shrinking core) picture of the network model is proposed. Information from adsorption-desorption equilibria are used to compute the thickness of the shell in which desorption/evaporation occurs for concentrations higher than the percolation threshold x^T. For concentrations lower than x^T, the model similar to the model for adsorption is used.

(3) Complete sets of experimental kinetic data for the systems silica gel-water vapor and Vycor glass-nitrogen are measured and analyzed.

(4) The adsorption model successfully predicts the experimental data with a maximum in diffusivity. The desorption model correctly predicts the dependence of diffusivity with a minimum, but the quantitative agreement is not satisfactory due to a number of reasons.

(5) Improvement of the models is possible by including more transport mechanisms (such as flow of liquid conden-

sate, nucleation) and/or by allowing the diffusivities to be dependent on concentration and pore size.

(6) The two models proposed in this work represent a unification of the theories for equilibrium and kinetics for systems with hysteresis. Information on the adsorption-desorption equilibria is needed for the models for mass transport. A minimum number of adjustable parameters are used in the models.

Acknowledgments

We would like to thank A. H. Danzberger, P.E., for helpful discussion. The work was supported by National Science Foundation grant CTS-9520328.

Notation

a = amount adsorbed (g/g)
B = fraction of liquid filled pores, Eq. 12
D = diffusivity in the network of pores; effective Fickian or overall diffusivity
D_o = surface diffusivity or diffusivity at zero loading
$f(d)$ = distribution function, Eq. 8
$f(x)$ = equilibrium function, Eq. 3
q = site filling probability, Eq. 1
Q = probability, Eq. 13
R_1 = shell thickness
t = time

Subscripts

E = evaporation
F = flow of capillary condensate
S = surface diffusion
∞ = value at surface
$1, 2, \ldots, n$ = different pores

Superscripts

T = percolation threshold
o = initial value

Literature Cited

Abeles, B., L. F. Chen, J. W. Johnson, and J. M. Drake, ''Capillary Condensation and Surface Flow in Microporous Vycor Glass,'' *Israel J. Chem*., **31**, 99 (1991).

Benzoni, J., and H. C. Chang, ''Effective Diffusion in Bi-disperse Media—An Effective Medium Approach,'' *Chem. Eng. Sci*., **39**, 167 (1984).

Broadbent, S. R., and J. M. Hammersley, ''Percolation Processes: I. Crystals and Mazes,'' *Proc. Camb. Phil. Soc*., **53**, 629 (1957).

Brunovská, A., J. Ilavsky, and H. Kukurucová, ''The Shell Progressive Model of Adsorption in a Single Particle,'' *Collect. Czechoslov. Chem. Commun*., **50**, 1341 (1985).

Burganos, V. N., and S. V. Sotirchos, ''Diffusion in Pore Networks: Effective Medium Theory and Smooth Field Approximation,'' *AIChE J*., **33**, 1678 (1987).

Büssing, W., H.-J. Bart, and R. Germerdonk, ''Isothermal Liquid Transport in Porous Media: Capillary Hysteresis Effects,'' *Int. J. Heat Mass Transfer*, **39**, 1925 (1996).

Burgess, C. G. V., D. H. Everett, and S. Nuttall, ''Adsorption Hysteresis in Porous Materials,'' *Pure Appl. Chem*., **61**, 1845 (1989).

Carman, P. C., ''Diffusion and Flow of Gases and Vapors Through Micropores: IV. Flow of Capillary Condensate,'' *Proc. R. Soc. London*, **A211**, 526 (1952).

Chen, Y. D., and R. T. Yang, ''Surface Diffusion of Multilayer Adsorbed Species,'' *AIChE J*., **39**, 599 (1993).

Daian, J.-F., ''From Pore-Size Distribution to Moisture Transport Properties: Particular Problems for Large Pore-Size Distributions,'' *Drying '92*, A. S. Mujumdar, ed., Elsevier, Amsterdam, 263 (1992).

Eberly, P. E., and D. B. Vosberg, ''Diffusion of Benzene and Inert Gases Through Porous Media at Elevated Temperatures and Pressures,'' *Trans. Faraday Soc*., **61**, 2724 (1965).

Everett, D. H., *Adsorption Hysteresis, The Solid-Gas Interface*, Vol. 2, E. A. Flood, ed., Marcel Dekker, New York, p. 1055 (1967).

Flood, E. A., R. H. Tomlinson, and A. E. Leger, ''The Flow of Fluids through Activated Carbon Rods III. The Flow of Adsorbed Fluids,'' *Can J. Chem*., **30**, 389 (1952).

Gilliland, E. R., R. F. Baddour, and J. L. Russell, ''Rates of Flow Through Microporous Solids,'' *AIChE J*., **4**, 90 (1958).

Gregg, S. J., and K. S. Sing, *Adsorption Surface Area and Porosity*, 2nd ed., Academic Press, London (1982).

Guyer, R. A., and K. R. McCall, ''Capillary Condensation, Invasion Percolation, Hysteresis, and Discrete Memory,'' *Phys. Rev. B*, **54**, 18 (1996).

Haynes, J. M., and R. J. Miller, ''Surface Diffusion and Viscous Flow During Capillary Condensation,'' *Adsorption at the Gas-Solid and Liquid-Solid Interface*, J. Rouquerol and K. S. W. Sing, eds., Elsevier, Amsterdam, p. 439 (1982).

Heinrichs, J., and N. Kumar, ''Simple Exact Treatment of Conductance in a Random Bethe Lattice,'' *J. Phys. C.: Solid State Phys.*, **8**, L510 (1975).

Kainourgiakis, M. E., E. S. Kikkinides, A. K. Stubos, and N. K. Kanellopoulos, ''Adsorption-Desorption Gas Relative Permeability through Mesoporous Media—Network Modelling and Percolation Theory,'' *Chem. Eng. Sci*., **53**, 2353 (1998).

Kapoor, A., R. T. Yang, and C. Wong, ''Surface Diffusion,'' *Catal. Rev. Sci. Eng*., **31**, 129 (1989).

Kärger, J., and D. M. Ruthven, *Diffusion in Zeolites and Other Microporous Solids*, Wiley, New York (1992).

Kirkpatrick, S., ''Classical Transport in Disordered Media: Scaling and Effective Medium Theories,'' *Phys. Rev. Lett*., **27**, 1722 (1971).

Larson, R. G., and H. T. Davis, ''Conducting Backbone in Percolating Bethe Lattices,'' *J. Phys. C.: Solid State Phys*., **15**, 2327 (1982).

Laurindo, J. B., and M. Prat, ''Numerical and Experimental Network Study of Evaporation in Capillary Porous Media. Phase Distributions,'' *Chem. Eng. Sci*., **51**, 5171 (1996).

Lee, K. H., and S. T. Hwang, ''The Transport of Condensable Vapors Through a Microporous Vapor Glass Membrane,'' *J. Colloid Interf. Sci*., **110**, 544 (1986).

Lee, S. Y., and R. Aris, ''The Distribution of Active Ingredients in Supported Catalysts Prepared by Impregnation,'' *Cata. Rev.-Sci. Eng*., **27**, 207 (1985).

Li, J.-C., D. K. Ross, and M. J. Benham, ''Small-Angle Neutron Scattering Studies of Water and Ice in Porous Vycor Glass,'' *J. Appl. Cryst*., **24**, 794 (1991).

Li, X., and Y. C. Yortsos, ''Visualization and Simulation of Bubble Growth in Pore Networks,'' *AIChE J*., **41**, 214 (1995).

Lilly, M. P., P. T. Finley, and R. B. Hallock, ''Memory, Congruence, and Avalanche Events in Hysteretic Capillary Condensation,'' *Phys. Rev. Lett*., **71**, 4186 (1993).

Liu, H., L. Zhang, and N. A. Seaton, ''Analysis of Sorption Hysteresis in Microporous Solids Using a Pore Network Model,'' *J. Colloid Interf. Sci*., **156**, 285 (1993).

Maneval, J. E., M. J. McCarthy, and S. Whitaker, ''Studies of the Drying Process by NMR Imaging,'' *Drying*, Elsevier, Amsterdam, p. 170 (1991).

Markos, J., A. Brunovská, and J. Ilavsky, ''Modelling of Catalytic Reactors with Catalyst Deactivation: IV. Parameter Estimation of the Rate Equations of Heterogeneous Catalyst Deactivation,'' *Chem. Papers*, **41**, 375 (1987).

Mason, G., ''Determination of the Pore/Size Distribution and Pore-Space Interconnectivity of Vycor Porous Glass from Adsorption-Desorption Hysteresis Capillary Condensation Isotherms,'' *Proc. R. Soc. London*, **A415**, 453 (1988).

Naono, H., and M. Hakuman, ''Analysis of Porous Texture by Means of Water Vapor Adsorption Isotherm with Particular Attention to Lower Limit of Hysteresis Loop,'' *J. Coll. Interf. Sci*., **158**, 19 (1993).

Neimark, A. V., L. I. Kheifez, and V. B. Fenelonov, ''Theory of Preparation of Supported Catalysts,'' *Ind. Eng. Chem. Prod. Res. Dev*., **20**, 439 (1981).

Page, J. H., J. Liu, B. Abeles, H. W. Deckman, and D. A. Weitz, ''Pore-Space Correlations in Capillary Condensation in Vycor,'' *Phys. Rev. Lett*., **71**, 1216 (1993).

Parlar, M., and Y. C. Yortsos, ''Percolation Theory of Vapor Ad-

sorption-Desorption Processes in Porous Materials,'' *J. Colloid Interf. Sci*., **124**, 162 (1988).
Parlar, M., and Y. C. Yortsos, ''Nucleation and Pore Geometry Effects in Capillary Desorption Processes in Porous Media,'' *J. Colloid Interf. Sci*., **132**, 425 (1989).
Pel, L., H. Brocken, and K. Kopinga, ''Determination of Moisture Diffusivity in Porous Media Using Moisture Concentration Profiles,'' *Int. J. Heat Mass Transfer*, **39**, 1273 (1996).
Prat, M., ''Percolation Model of Drying under Isothermal Conditions in Porous Media,'' *Int. J. Multiphase Flow*, **19**, 691 (1993).
Prat, M., ''Isothermal Drying of Non-Hydroscopic Capillary—Porous Materials as an Invasion Percolation Process,'' *Int. J. Multiphase Flow*, **21**, 875 (1995).
Radjy, F., ''Moisture Transport in Microporous Substances,'' *J. Mat. Sci*., **9**, 744 (1974).
Rajniak, P., ''Analysis of a One-Component Sorption in a Single Adsorbent Particle by the Orthogonal Collocation Method. IV. One-Point Collocation Method and Linear Driving-Force Approximation,'' *Chem. Papers*, **39**, 447 (1985).
Rajniak, P., and R. T. Yang, ''A Simple Model and Experiments for Adsorption-Desorption Hysteresis: Water Vapor on Silica Gel,'' *AIChE J*., **39**, 774 (1993).
Rajniak, P., and R. T. Yang, ''Hysteresis-Dependent Adsorption-Desorption Cycles: Generalization for Isothermal Conditions,'' *AIChE J*., **40**, 913 (1994).
Rajniak, P., and R. T. Yang, ''Unified Network Model for Diffusion of Condensable Vapors in Porous Media,'' *AIChE J*., **42**, 319 (1996).
Rhim, H., and S. T. Hwang, ''Transport of Capillary Condensate,'' *J. Coll. Interface Sci*., **52**, 174 (1975).
Sahimi, M., ''Nonlinear Transport Processes in Disordered Media,'' *AIChE J*., **39**, 369 (1993).
Sahimi, M., *Applications of Percolation Theory*, Taylor and Francis, London (1994).
Sahimi, M., *Flow and Transport in Porous Media and Fractured Rock*, VCH Verlagsgesellschaft mbH, D-69451 Weinheim (1995).
Sahimi, M., G. R. Gavalas, and T. T. Tsotsis, ''Statistical and Continuum Models of Fluid-Solid Reaction in Porous Media,'' *Chem. Eng. Sci*., **45**, 1443 (1990).
Seaton, N. A., ''Determination of the Connectivity of Porous Solids from Nitrogen Sorption Measurements,'' *Chem. Eng. Sci*., **46**, 1895 (1991).
Stauffer, D., and A. Aharony, *Introduction to Percolation Theory*, 2nd ed., Taylor and Francis, London (1992).
Stinchcombe, R. B., ''Conductivity and Spin-Wave Stiffness in Disordered Systems—An Exactly Soluble Model,'' *J. Phys. C.: Solid State Phys*., **7**, 179 (1974).
Tamon, H., M. Okazaki, and R. Toei, ''Flow Mechanism of Adsorbate Through Porous Media in Presence of Capillary Condensation,'' *AIChE J*., **27**, 271 (1981).
Toei, R., H. Imakoma, H. Tamon, and M. Okazaki, ''Water Transfer Coefficient in Adsorptive Porous Body,'' *J. Chem. Eng. Japan*, **16**, 364 (1983).
Uhlhorn, R. J. R., K. Keizer, and A. J. Burgraaf, ''Gas Transport and Separation with Ceramic Membranes I. Multilayer Diffusion and Capillary Condensation,'' *J. Memb. Sci*., **66**, 259 (1992).
Villadsen, J., and M. L. Michelsen, *Solution of Differential Equation Models by Polynomial Approximation*, Prentice Hall, Englewood Cliffs, NJ (1978).
Weisz, P. B., ''Diffusion Transport in Chemical Systems—Key Phenomena and Criteria, Berichte der Bunsen-Gesselschaft,'' *Phys. Chem*., **79**, 798 (1975).
Wilkinson, D., and J. F. Willemsen, ''Invasion Percolation: A New Form of Percolation Theory,'' *J. Phys. A*, **16**, 3365 (1983).
Yang, R. T., *Gas Separation by Adsorption Processes*, Butterworth, Boston (1987) [in paperback, Imperial College Press and World Scientific Publishers, River Edge, NJ (1997)].
Yortsos, Y. C., C. Satik, J.-C. Bacri, and D. Salin, ''Large-Scale Percolation Theory of Drainage,'' *Transport in Porous Media*, **10**, 171 (1993).

Manuscript received Sept. 2, 1998, and revision received Jan. 19, 1999.